Available online at www.sciencedirect.com
SCIENCE DIRECT
Polymer 45 (2004) 6037–6044
polymer
www.elsevier.com/locate/polymer

# Dependence of the network structure of cured styrene butadiene rubber on the sulphur content

W. Salgueiro[a], A. Marzocca[c], A. Somoza[a,b,*], G. Consolati[d], S. Cerveny[c,e], F. Quasso[d], S. Goyanes[c,e]

[a]*IFIMAT-UNCentro, Pinto 399, B7000GHG Tandil, Argentina*
[b]*Comisión de Investigaciones Científicas de la Provincia de Buenos Aires, Calle 526 e loy 11, 1900 La Plata, B7000GHG Tandil, Argentina*
[c]*LPMPyMC, Departamento de Física, Facultad de Ciencias Exactas y Naturales, Universidad Nacional de Buenos Aires, Ciudad Universitaria, Pabellon I, (1428) Buenos Aires, Argentina*
[d]*Consejo Nacional de Investigaciones Científicas y Tecnológicas, Argentina*
[e]*Istituto Nazionale di Fisica della Materia and Dipartimento di Fisica, Politecnico di Milano, Piazza Leonardo da Vinci 32, I-20133 Milano, Italy*

Received 17 February 2004; received in revised form 14 April 2004; accepted 4 May 2004

Available online 10 July 2004

**Abstract**

An investigation about the dependence of the physical properties of styrene–butadiene rubber copolymers (cured with different sulphur content, in order to obtain various networks) on the crosslink density was carried out by means of dynamical mechanical analysis, differential scanning calorimetry and positron annihilation lifetime spectroscopy. SBR specimens were cured with different sulphur content, in order to obtain various networks. On increasing the crosslink density, the glass transition temperature increases and the fractional free volume decreases. The thermal expansion coefficient of the free volume decreases in the rubbery phase by increasing the crosslink density, owing to the slower rate of expansion of nanoholes; furthermore, it seems influenced by the percentage of polysulfide density. The density of nanoholes is independent of the temperature, but decreases on adding sulphur. The results can be framed within the Simha–Somcynsky free volume theory.


*Keywords:* Nanohole; SBR copolymer; Free volume

## 1. Introduction

The effects of the sulphur content on the mechanical, thermal and electrical properties of styrene–butadiene rubber (SBR) compounds are well documented [1–3]; indeed, crosslinking has a strong influence on the physical properties of polymers and in particular on the free volume. This last concept, initially introduced to account for the dependence of the viscosity on the temperature in simple liquids [4] and subsequently extended to polymeric systems [5], turns out to be useful to explain many mechanical and viscoelastic properties of macromolecules. Various experimental techniques have been used to get information on the free volume: photochromic labels [6], $^{129}$Xe NMR [7], electron spin resonance [8] and small angle X-ray scattering [9]; among them, positron annihilation lifetime spectroscopy (PALS) has gained increasing popularity as a non-destructive tool [10]. It is based on the fact that positronium (Ps), the positron–electron bound system, is repelled from the ionic cores of the atoms and molecules due to exchange interactions and tends to localize into the nanohole volumes; its lifetime can be related to the average size of the holes through a semiempirical equation [11,12]. Therefore, it is possible to obtain the main features of the free volume as well as its changes (induced, e.g., by temperature) by studying Ps annihilation in a polymer.

In a recent paper [13] some of us investigated the effect of the cure on the free volume of a specific SBR (SBR 1502) by means of PALS and dynamical mechanical analysis (DMA), using sulphur and an accelerator as vulcanization system. It was shown that the lowest free volume was observed at the beginning of the networking process; then, it

* Corresponding author. Address: Instituto de Fisica de Materiales Tandil, Fisica, Pinto 399, 7000 Tandil, Argentina. Tel.: +54-229344-2821; fax: +54-229344-4190.
*E-mail address:* asomoza@exa.unicen.edu.ar (A. Somoza).

0032-3861/$ - see front matter © 2004 Published by Elsevier Ltd.
doi:10.1016/j.polymer.2004.05.008

slowly increased up to an equilibrium value, reached when the polymer was fully cured.

In the present paper, the analysis was pursued with the aim to study the influence of the sulphur content, that is, of the crosslink density, on the structure of an SBR copolymer; in particular, interest was focused on the free volume. Indeed, by varying the amount of sulphur, concentration of crosslink due to sulfide linkages between carbon atoms of the polymer chain can be adjusted [14]. The experimental results were framed within the Simha–Somcynsky theory [15], which produced one of the most fruitful equation of state for polymers. Behavior of the investigated structures predicted by the theory was compared to PALS data, in order to obtain meaningful free volume quantities, such as the nanovoid density or the free volume fraction at the glass transition temperature.

## 2. Experimental method

### 2.1. Samples preparation

The material was unfilled styrene butadiene rubber SBR-1502 that contains 23.5% bound styrene, i.e., a molecular proportion in the chains of one styrene to about six or seven butadienes. The chemical structure of butadiene in the SBR copolymer consists of 55% *trans*-1,4, 9.5% *cis*-1,4 and 12% 1,2-butadiene.

The average molecular weight of the elastomer was $M_n = 176,000$ g/mol as determined by gel permeation chromatography, with a density $\rho = 0.935$ g/cm$^3$. To obtain different network structures, three formulations based on the system of cure sulphur/TBBS (*N*-*t*-butyl-2-benzothiazole sulfenamide) were prepared by varying the amount of sulphur. The recipes are given in Table 1.

The blends, prepared in a laboratory mill, were characterized at 433 K by means of the torque curves in a Monsanto MDR2000 rheometer. These curves are given in Fig. 1. From these curves, the time to achieve the maximum torque, $t_{100\%}$, was calculated in each sample and is given in Table 1.

Sample sheets of $150 \times 150 \times 2$ mm$^3$ were vulcanized at 433 K for a time interval equal to $t_{100\%}$, in order to guarantee that the vulcanization reaction was completed. These specimens were rapidly cooled in an ice-water bath at the end of the curing cycle. The density of each sample is also given in Table 1.

Table 1
Compound formulations (in phr), density, and $t_{100\%}$

| | Sample a | Sample b | Sample c |
|---|---|---|---|
| SBR 1502 | 100 | 100 | 100 |
| Zinc oxide | 5 | 5 | 5 |
| Stearic acid | 2 | 2 | 2 |
| Antioxidant | 1.2 | 1.2 | 1.2 |
| Accelerator (TBBS) | 1.2 | 1.2 | 1.2 |
| Sulfur (S) | 0.9 | 1.8 | 5.4 |
| $\Lambda$ (accelerator/S ratio) | 1.33 | 0.66 | 0.22 |
| $t_{100\%}$ (min) | 33.7 | 28.3 | 22.1 |
| Density (g/cm$^3$) | 0.980 | 0.988 | 1.003 |

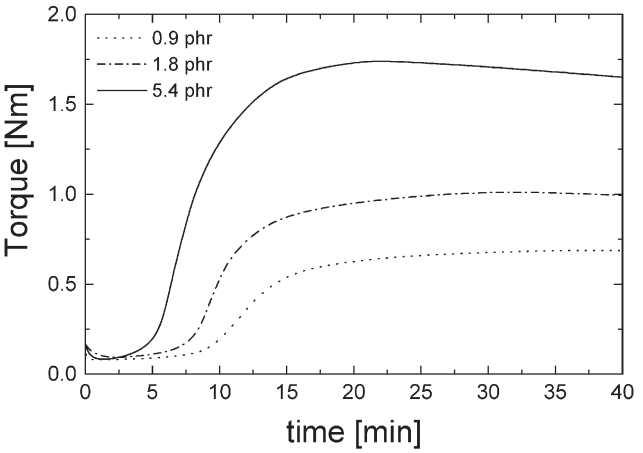


Fig. 1. Torque curves characterized at 433 K as a function of time.

### 2.2. Swelling tests

Swelling of rubber compounds is frequently used for the determination of the crosslink density. The density of chemical crosslinks was determined using the method described by Cunneen and Russell [16].

The molecular weight of the network chain between chemical crosslinks for a phantom network, $M_{cs}$, is expressed by the Flory–Rehner relationship [17,18]:

$$M_{cs} = -\frac{\rho(1 - 2/\phi)V_1 v_{2m}^{1/3}}{\ln(1 - v_{2m}) + \chi v_{2m}^2 + v_{2m}} \quad (1)$$

where $\rho$ is the density of the rubber network, $\phi$ the functionality of the crosslinks, $v_{2m}$ the volume fraction of polymer at equilibrium (maximum) degree of swelling and $V_1$ the molar volume of solvent. $\chi$ is an interaction parameter between the polymer and the swelling agent [19].

Samples of 16 mm diameter were cut with a die from the cured sheets for each compound. Each sample was completely immersed in a solvent until equilibrium swelling occurred. The initial weight was $10^{-4}$ g for all the samples. Then the total number of crosslinks was determined by weighting the samples. The solvent used was toluene ($\rho_{tol} = 0.8669$ g/cm$^3$, $V_1 = 106.29$ ml/mol) [20]. The polymer–solvent interaction parameter $\chi$ for the system SBR–toluene [21] was 0.446.

The concentration of the polysulfide crosslinks was evaluated from the change in the crosslink density of the cured samples before and after treatment with a solution of piperidine and propane-2-thiol [16], which cleaves the polysulphide crosslinks when the sample remains for 2 h in this solution.

Similarly, the concentration of the monosulfide cross-

links was evaluated from the change in the crosslink density of the cured samples before and after treatment with a solution of piperidine and *n*-hexanethiol [16].

Finally, the density of disulfide crosslinks was calculated from the difference between the total crosslink density and the addition of the polysulfides and monosulfides crosslink densities previously determined.

### 2.3. Positron spectroscopy

A fast–fast timing coincidence system with two $BaF_2$ scintillator detectors was used as lifetime spectrometer for the PALS measurements, having a time resolution (FWHM) of about 380 ps. The positron lifetime spectra were recorded in the temperature range from 180 to 340 K. For this aim, a liquid Nitrogen cryostat (DN1714 Oxford Instruments) was used, which ensured a stability of the temperature within 0.3 K. The source was placed between two identical square-shaped samples of 2 mm thick and 15 mm side obtained from the same sheets used for dynamic mechanical test. The samples were introduced into a Cu sample holder and this last was inserted in the cryostat. The activity of the positron source ($^{22}$Na deposited onto a Kapton foil 7.5 μm thick) was about $2 \times 10^5$ Bq. Each spectrum contained about $3 \times 10^6$ annihilation events. Spectra were deconvoluted by using the POSITRONFIT code [22].

### 2.4. Dynamic mechanical and DSC measurements

Dynamic mechanical test were performed in the samples by using a Rheometrics DMA IV in the traction mode at 1 Hz, in the temperature range between 200 and 273 K at a scanning rate of 1 K/min. Samples were cut with a die. The dimensions of the samples were 15 mm × 5 mm × 2 mm. The storage modulus ($E'$), loss modulus ($E''$) and loss tangent (tan δ) were evaluated for each sample.

DSC thermal measurements were performed with a Mettler-Toledo 822 instrument, indium and zinc calibrated. Samples of about 15 mg were heated from 193 to 298 K at a scanning rate of 10 K/min, in nitrogen atmosphere.

## 3. Results and discussion

Fig. 1 shows the rheometer curves of each sample. As expected, the maximum torque reached during the tests increases with the sulphur content in the compound, due to the increase in the active crosslink concentration. Our measurements of swelling confirm this assumption. Indeed, the crosslink density in a 4-functional network is defined by [23]:

$$\mu_c = \frac{\rho}{2}\left(\frac{1}{M_{cs}} - \frac{1}{M_n}\right) \quad (2)$$

where $\rho$ is the density of the polymer. From Eq. (2) $\mu_c$ was evaluated for each sample. First, the molecular weight was calculated between crosslinks for the original samples; secondly, it was calculated when the polysulfide crosslinks were cleaved after the treatment with piperidine and propane-2-thiol and, once more, when the polysulfide an disulfide crosslinks were cleaved after treatment with piperidine and *n*-hexanethiol. The values of $M_{cs}$ are given in Table 2.

The variation of the total crosslink density with the sulphur content in each compound is shown in Fig. 2. The polysulfide, disulfide and monosulfide crosslink densities in each sample are also given: the total crosslink density increases with the sulphur content. The proportion of polysulfides in the sample with 5.4 phr of sulphur is less than those corresponding to the other two samples. There is also an increase in monosulfides crosslink density for the sample with higher sulphur content.

Glass transition temperature of the samples was investigated by dynamical mechanical analysis and differential scanning calorimetry. In Fig. 3 the variation of the dynamic moduli, storage modulus ($E'$), loss modulus ($E''$) and loss factor (tan δ) obtained at a frequency of 1 Hz versus temperature is given. $E'$ increases with the degree of crosslinking in the rubbery as well as in the glassy region of the curves. Both $E''$ and tan δ show a maximum that can be attributed to the glass transition temperature $T_g$. The $T_g$ from the maximum of $E'$ occurs close to the initial drop of the storage modulus from the glassy to the transition zone and this fact is correlated to the onset of a change in mechanical properties of the compound [24].

The estimated values of $T_g$ as a function of the crosslink density for each SBR compound obtained by DMA, DSC and PALS are shown in Fig. 4. An increase in $T_g$ can be

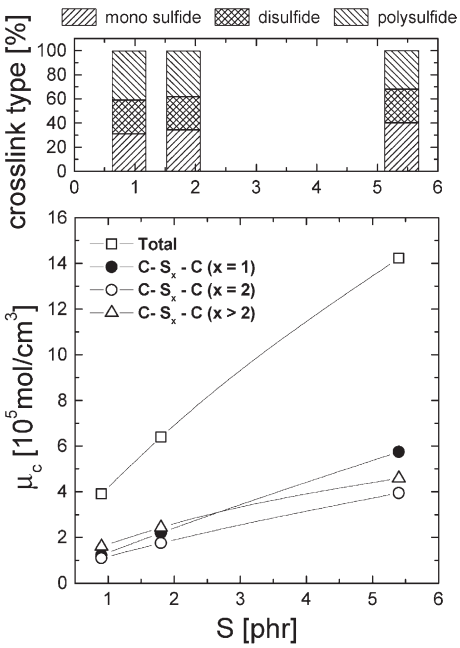


Fig. 2. Lower panel: variation of the total crosslink density versus sulphur content. Upper panel: percentage of the three crosslink types (di-, mono- or polysulfide) in the investigated samples.

Table 2
Molecular weight of the network chain between the chemical crosslinks $M_{cs}$

| | $M_{cs}$ (g/mol) orginal network | $M_{cs}$ (g/mol) After treatment with piperidine and propane-2-thiol | $M_{cs}$ (g/mol) after treatment with piperidine and *n*-hexanethiol |
|---|---|---|---|
| Sample a | 11,207 | 18,768 | 35,604 |
| Sample b | 7023 | 11,303 | 20,367 |
| Sample c | 3219 | 4741 | 8016 |

observed by increasing the crosslink density. The glass transition temperature from the DMA technique was obtained by using the data shown in Fig. 3. Concerning DSC analyses, the glass transition temperature was evaluated as the inflection point of the heat flow curve versus temperature. Fig. 4 also shows $T_g$ as obtained by PALS; the method is described below. Whatever the technique used, the values of $T_g$ increase by increasing the crosslink density, according to the expectations; furthermore, Fig. 3 shows that the width of the tan $\delta$ peak increases with the crosslink density, as well. This is probably due to the presence of heterogeneous microregions which relax over a range of temperatures; the width of such temperature interval increases with the crosslinking.

Positron annihilation lifetime spectra were deconvoluted into three discrete components; a suitable correction for the positrons annihilated in the source support was taken into account. According to the common interpretation for PALS measurements in polymers we ascribed the longest component to ortho-Ps decay in the nanocavities forming the free volume. The intermediate component (0.35–0.50 ns) is attributed to positrons annihilated in low electron density regions of the structure. The shortest component (0.15–0.23 ns) is due to positrons annihilated in the bulk and to para-Ps annihilations; this last contribution cannot be resolved as a distinct component.

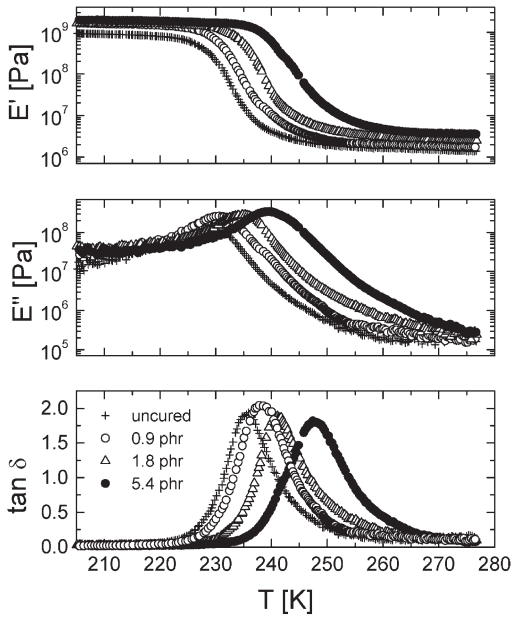


Fig. 3. Storage modulus ($E'$), loss modulus ($E''$) and loss factor (tan $\delta$) versus temperature. All the dynamic moduli were obtained at a frequency of 1 Hz.

The behavior of the longest-lived lifetime $\tau_3$ with the temperature for the various samples is shown in Fig. 5. A similar trend for all the samples is observed, with a systematic shift to lower values when the sulphur content increases. In all the curves, three temperature regions can be distinguished: the low and high temperature regions ($T \leq 220$ K and $T \geq 300$ K, respectively) where there is a moderate variation of $\tau_3$ with $T$, and the 'intermediate' region where a sharp increase of the rate of variation of $\tau_3$ with $T$ is evidenced. The change of $\tau_3$ from the low to the intermediate region corresponds to the glass transition. The glass transition temperature $T_g$ was obtained as the intersection point of the two straight lines fitting the data at low and intermediate temperatures. Relative errors on $T_g$ arising from the uncertainties of $\tau_3$ are estimated to be about 8%. These data were included in Fig. 4 and in Table 3. $T_g$ values obtained from $\tau_3$ in the PALS experiments have lower values than those obtained by DSC or DMA. This depends on the fact that $T_g$ is not a thermodynamic property but a kinetic one and its value is influenced by the heating rate both in DSC and DMA tests. Times required for carrying out PALS measurements are much longer than those necessary for thermal tests and this can explain the lower values for $T_g$ obtained by PALS. Furthermore, in PALS measurements the glass transition is related to the

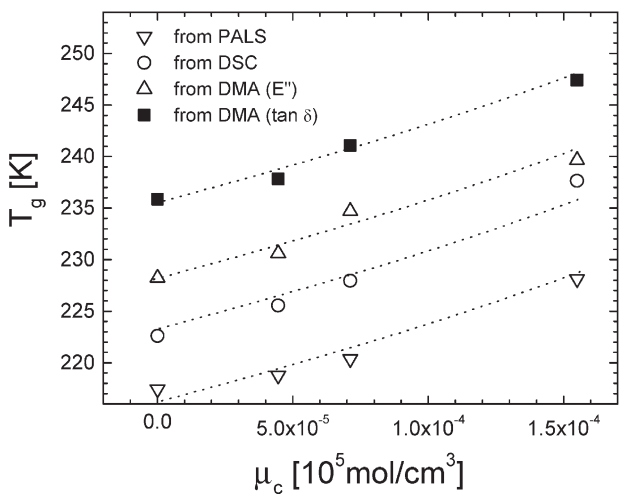


Fig. 4. Glass transition temperature $T_g$ versus crosslink density as obtained by various techniques.

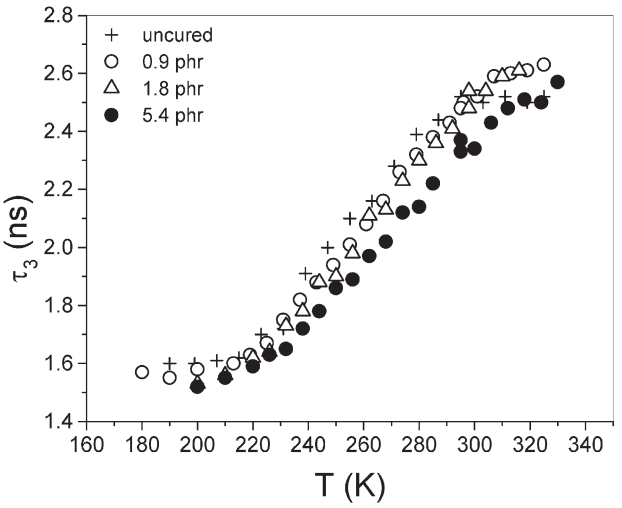


Fig. 5. ortho-Positronium lifetime $\tau_3$ versus temperature in the investigated samples.

change in the amplitude of movements of very short polymer segments which are involved in the thermal processes of the hole formation. These processes begin at temperatures lower than those involved in the $T_g$ evaluations by DSC, which is related to a change of the heat capacity of the polymer.

Various explanations were proposed for the reduced increase of $\tau_3$ at the highest temperatures: formation of a Ps bubble in the liquid phase, digging of holes by Ps itself [25] or relaxation time of the molecular chains [26] comparable to $\tau_3$ : in this case Ps is no longer able to correctly probe the sizes of the nanovoids trapping it. Independent of the adopted explanation, there is a general agreement on the contention that o-Ps in this temperature region does not give correct information on the free volume. In the subsequent discussion this region will no longer be considered.

Concerning ortho-Ps intensity $I_3$, it does not depend on the temperature, but assumes a constant value (within the experimental errors) which depends on the sulphur content: $I_3$ decreases when the crosslink density increases, as shown in Table 3. In the case of the uncured sample, the corresponding $I_3$ value is below those obtained for samples having 0.9 and 1.8 phr sulphur content.

Lifetime data can be transformed into average sizes of the free volume holes by using the Tao–Eldrup semiempirical equation [11,12]: the cavity hosting Ps is assumed to be a spherical void with effective radius $R$. Such a Ps trap has a potential well with finite depth; however, for convenience of calculations one usually assumes the depth as infinite, but the radius increased to $R + \Delta R$, $\Delta R$ (0.166 nm) [12] being an empirical parameter which describes the penetration of Ps wave function into the bulk. The electron density is supposed to be zero for $r < R$ and constant for $r > R$. The relationship between o-Ps lifetime $\tau_3$ (ns) and radius $R$ is the following [11,12]:

$$\tau_3 = 0.5\left[\frac{\Delta R}{R+\Delta R} + \frac{1}{2\pi}\sin\left(2\pi\frac{R}{R+\Delta R}\right)\right]^{-1} \quad (3)$$

Of course, the values of the radii obtained from Eq. (3) should be interpreted only as rough estimates, since real holes are irregularly shaped. Average volume of holes $v_3 = v_h = 4/3\pi R^3$ as obtained from Eq. (3) are shown in Fig. 6; they are a key quantity to evaluate the free volume. This last is defined as:

$$V_f = N' v_h \quad (4)$$

where $N'$ is the density of holes. Various approaches were used to get the fractional free volume from positron data. The following equation is still popular [27]:

$$f_v = C I_3 v_h \quad (5)$$

where $C$ is a constant and $I_3$ is o-Ps intensity. It is based on the hypothesis that $I_3$ is proportional to $N'$. Although appealing for its simplicity, Eq. (5) should be cautiously considered since it is a pure phenomenological relationship; it was heavily criticized [28] since several factors simultaneously concur to Ps formation and it is generally impossible among them to isolate the influence of the hole density. In the present work we will use Eq. (4).

To get information on $N'$ we followed the method used in Ref. [29]; specific volume is written as:

$$V = V_f + V_{occ} = N' v_h + V_{occ} \quad (6)$$

where $V_{occ}$ is the occupied volume and the free volume $V_f$ is given by Eq. (4). Fractional free volume is therefore:

$$f = \frac{V_f}{V} = \frac{N' v_h}{N' v_h + V_{occ}} \quad (7)$$

To obtain the specific volume $V$ we used the Simha–Somcynsky equation of state for polymers [15] at atmospheric pressure, which can be approximated by the

Table 3
$T_g$ measured by PALS, scaling temperature $T^*$, hole density $N'$, average o-Ps intensity $I_3$, fractional free volume at $T_g$, $f(T_g)$, occupied volume $V_{occ}$ and thermal expansion free volume coefficients in the rubbery ($\alpha_r$) and in the glassy ($\alpha_g$) phases

| Sample | $T_g$ (K) | $T^*$ (K) | $N'$ $10^{-21}$ ($g^{-1}$) | $I_3$ (%) | $f(T_g)$ | $V_{occ}$ ($cm^3\ g^{-1}$) | $\alpha_r \times 10^4$ ($K^{-1}$) | $\alpha_g \times 10^4$ ($K^{-1}$) |
|---|---|---|---|---|---|---|---|---|
| Uncured | 219 | 7164 | 0.79 | 19.4 | 5.3 | 0.945 | 8.6 | 0.5 |
| a | 221 | 8621 | 0.61 | 20.6 | 4.0 | 0.929 | 6.7 | 0.6 |
| b | 222 | 8938 | 0.57 | 20.2 | 3.7 | 0.929 | 6.4 | 1.4 |
| c | 229 | 9628 | 0.60 | 12.0 | 3.9 | 0.921 | 5.8 | 1.5 |

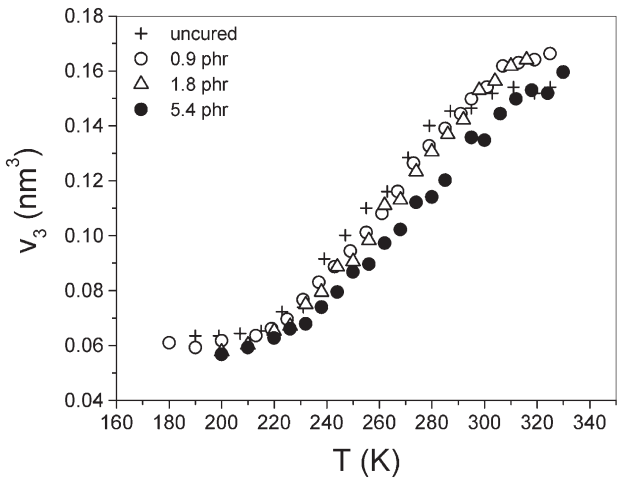


Fig. 6. Average hole volumes (in spherical approximation) versus temperature for the investigated samples.

following universal scaling relationship [30] for $T > T_g$ :

$$\ln\frac{V}{V^*} = a + b\left(\frac{T}{T^*}\right)^{3/2} \quad (8)$$

where $a = -0.1033$ and $b = 23.835$ are universal constants; $V^*$ and $T^*$ are scaling parameters, dependent on the specific structure of polymer. Concerning $V^*$, it results, with a very good approximation, $V^* = 1.45V_W$, where $V_W$ is the Van der Waals volume [31]. In the case of the uncured SBR studied in this work, we computed $V_W = 0.672\ \mathrm{cm^3\ g^{-1}}$; it follows that $V^* = 0.974\ \mathrm{cm^3\ g^{-1}}$ and we used this value for all the investigated samples, since curing introduces only slight modifications. Knowledge of $V^*$ allows one to find $T^*$ from Eq. (8) by means of a single measurement of the density $\rho$ (Table 1) at room temperature: indeed, $V = 1/\rho$. Values of $T^*$ are shown in Table 3. Then, the behavior of specific volume versus temperature is obtained again using Eq. (8).

According to Eq. (7), $V$ can be plotted as a function of $v_h$ for the investigated polymers,; the results are shown in Fig. 7. We only need $V_{occ} = KV^*$, where $K$ is a very weakly temperature-dependent coefficient whose values are tabulated in Table 4 for the range of temperatures of interest [32]. The specific volume shows a linear dependence with $v_h$; correlation coefficients are always higher than 0.97. It follows that $N' = \text{const.}$, according to previous findings [29]. We note that we could still write Eq. (6) also for $N' \neq \text{const.}$, but the relationship between $V$ and $v_h$ would be no longer linear. Values of $N'$ are shown in Table 3. We remark that the guess represented by Eq. (5) is not in agreement with the present results; indeed, the behavior of $I_3$ (also shown in Table 3) versus the content of sulphur is rather different from that of $N'$. A further check of the procedure here adopted is given by the intercepts of the straight lines plotted in Fig. 7, which represent the occupied volume experimentally determined. They are shown in Table 3 and their average is in very good agreement with the value obtained by the theory ($0.931\ \mathrm{cm^3\ g^{-1}}$).

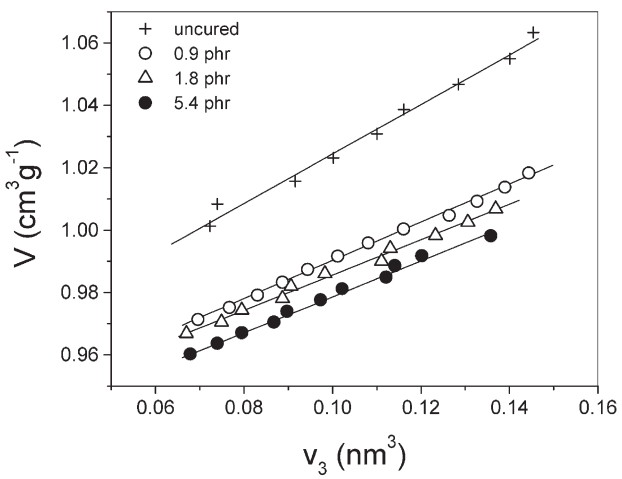


Fig. 7. Specific volume $V$ versus the hole volume $v_h$ for the investigated samples.

Fractional free volume $f$ as function of the temperature can be calculated using Eq. (7) and it is shown in Fig. 8. We used Eq. (7) also in the glassy state, by assuming for $N'$ the same value found above $T_g$. In Table 3 the values of $f(T_g)$ are collected; they are clearly different each other, in agreement with the contention that $T_g$ is $n/t$ an iso-free-volume state [33]. By increasing the crosslink density of the samples, a decrease in the fractional free volume occurs, which means an increased packing density in the rubbery phase; this is reasonable, since the higher constraints on the polymer due to the network hinder the thermal mobility of the chains. This effect is not so pronounced in the glassy region, since the thermal mobility is almost frozen and reduced effects are expected in the free volume. Similar results were obtained in *cis*-polyisoprene and high vinyl-polybutadiene [29] as well as in an amine-cured epoxy thermosetting polymer [27,34]. However, in another amine-cured epoxy [35] a non-monotonic relationship between free volume and crosslink density was found. Therefore, the results cannot be immediately generalized.

Concerning the thermal expansion coefficient of the free volume, $\alpha = \mathrm{d}f/\mathrm{d}T$, it shows a constant decrease by increasing the crosslink density in the rubbery phase ($\alpha_r$, Table 3). This means that in the rubbery phase the thermal expansion of the polymer is slower, the higher is the crosslink density, which can be expected by considering that the presence of the network limits the mobility of polymeric chains. Apparently, the behavior of $\alpha$ is opposite in the

Table 4
Values of the scaled occupied volume $K$ for the range of temperatures of interest

| $T$ (K) | $K$ |
|---|---|
| 225 | 0.917 |
| 246 | 0.918 |
| 266 | 0.918 |
| 285 | 0.919 |

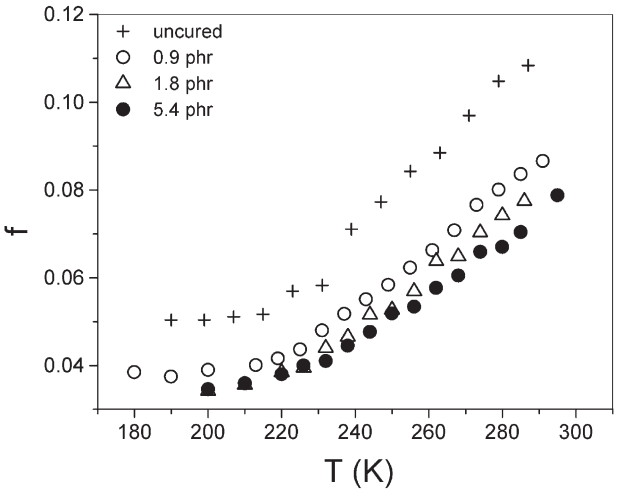


Fig. 8. Fractional free volume $f$ versus the temperature in the investigated samples.

glass, although in this case experimental uncertainties are higher.

Fig. 9 shows the thermal expansion coefficient of the free volume in the rubbery phase normalized to the total crosslink density, $\alpha_r/\mu_c$, versus the ratio between the polysulphide crosslink density and the monosulphide crosslink density. In fact, as already shown in Fig. 2, the contribution (percentage) of disulphide crosslink density is the same for all the cured samples. It is clear that the presence of polysulphide crosslink density in the samples increases the value of $\alpha_r/\mu_c$. Although a definite conclusion cannot be drawn due to the small number of investigated samples, it seems that the thermal expansion of the free volume is affected by the ratio between the different kinds of crosslink in the compound. Work is in progress to shed light on this subject.

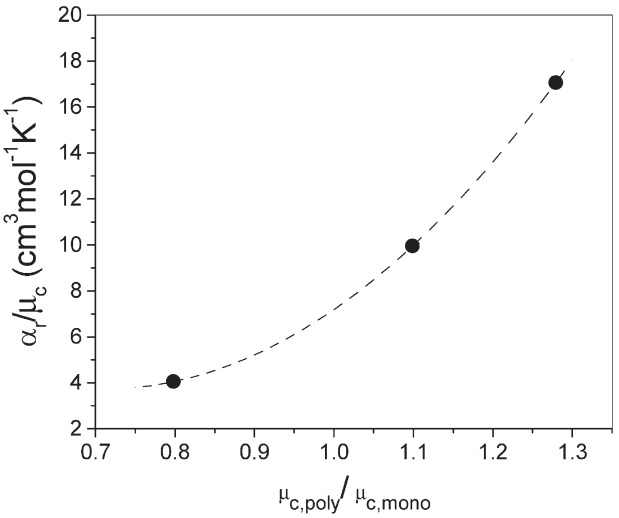


Fig. 9. Thermal expansion coefficient of the free volume for $T > T_g$, normalized to the total crosslink density, versus the ratio between mono-to-polysulfide crosslink density.

## 4. Conclusions

The measurements above discussed are compatible with other results reported on crosslinked structures. In particular, we found that the free volume at the glass transition temperature decreases by increasing the crosslink density and this was attributed to a lower density of nanoholes $N'$, since their average volume remains rather constant. On the other hand, such volume expands slower with the temperature when crosslinking increases, while nanohole density does not depend on the temperature.

ortho-Ps intensity $I_3$ does not depend on the temperature, either; however, its dependence on the content of sulphur is different with respect to $N'$. This fact casts shadows on the correctness of the proportionality between $I_3$ and $N'$.

Thermal expansion coefficient of the free volume seems to change with the composition of the sulfides forming the network. On increasing the percentage of polysulfides with respect to monosulfides the thermal expansion coefficient increases, while the crosslink density maintains constant. However, this subject needs to be investigated more thoroughly.

Finally, we remark that the experimental results obtained through PALS are well framed within the Simha–Somcynsky theory of the free volume.

## Acknowledgements

This work was supported by Consejo Nacional de Investigaciones Científicas y Técnicas (PIP N° 02825/01), Comisión de Investigaciones Científicas de la Provincia de Buenos Aires, Secretaría de Ciencia y Técnica (UNCentro), University of Buenos Aires (Project UBACYT X-150) and Fundación Antorchas, Argentina. G.C. acknowledges the support by the Ministero dell'Istruzione, dell'Università e della Ricerca through the MIUR-Cofin 2002 project (prot. n. 2002033184_005). O. Toscano and M.T. Maldonado are acknowledged by their technical assistance.

## References

[1] Payne AR. In: Kraus G, editor. Reinforcement of elastomers. New York: Interscience; 1965. p. 64.
[2] Marzocca AJ, Goyanes SN. J Appl Polym Sci 2004;91:2601.
[3] Abd-El-Messieh SL, Abd-El-Nour KN. J Appl Polym Sci 2003;88:1613.
[4] Doolittle AK. J Appl Phys 1951;22:1031.
[5] Ferry JD. Viscoelastic properties of polymers, 3rd ed. New York: Wiley; 1980.
[6] Victor JG, Torkelson JM. Macromolecules 1987;20:2241.
[7] Suzuki T, Yoshimizu H, Tsujita Y. Polymer 2003;44:2975.
[8] Bruno GV, Freed JH. J Phys Chem 1974;78:935.
[9] Curro JJ, Roe RR. Polymer 1984;25:1424.
[10] Dlubek G, Fretwell HM, Alam MA. Macromolecules 2000;33:87.
[11] Tao SJJ. Chem Phys 1972;56:5499.

[12] Eldrup M, Lightbody D, Sherwood N. J Chem Phys 1981;63:51.
[13] Marzocca AJ, Cerveny S, Salgueiro W, Somoza A, Gonzalez L. Phys Rev E 2002;65:021801.
[14] Coran AY. In: Mark JE, Erman B, Eirich FR, editors. Science and technology of rubber. San Diego: Academic Press; 1978. p. 339.
[15] Simha R, Somcynsky T. Macromolecules 1969;2:342.
[16] Cunneen JI, Russell RM. Rubber Chem Technol 1970;43:1215.
[17] Flory PJ, Rehner J. J Chem Phys 1943;11:512.
[18] Flory PJ, Rehner J. J Chem Phys 1943;11:521.
[19] Mark JE, Erman B. Rubberlike elasticity: a molecular primer. New York: Wiley; 1988. p. 51.
[20] Lide DR, editor. CRC handbook of chemistry and physics, 78th ed. New York: CRC Press; 1997. p. 3–55.
[21] Deng JS, Isayev I. Rubber Chem Technol 1991;64:296.
[22] Kirkegaard P, Pedersen NJ, Eldrup M. PATFIT Program Risø-M-2740 RNL; Roskilde, Denmark; 1989.
[23] Gronsky W, Hoffman U, Simon G, Wutzler A, Straube E. Rubber Chem Technol 1992;65:63.
[24] Sircar AK. In: Turi EA, editor. Thermal characterization of polymeric materials. San Diego: Academic Press; 1997. p. 980.
[25] Ito Y, Mohamed HFM, Tanaka K, Okamoto K, Lee K. J Radioanal Nucl Chem, Articles 1996;211:211.
[26] Bartos J, Sausa O, Kristiak J, Blochowicz T, Rossler E. J Phys: Condens Matter 2001;13:11473.
[27] Wang YY, Nakanishi H, Yean YC, Sandreczki TC. J Polym Sci, Part B, Polym Phys 1990;28:1431.
[28] Wang CL, Hirade T, Maurer FJH, Eldrup M, Pedersen NJ. J Chem Phys 1998;108:4654.
[29] Srithawatpong R, Peng ZL, Olson BG, Jamieson AM, Simha R, McGerwey JD, Maier TR, Halasa AF, Ishida H. J Polym Sci, Part B, Polym Phys 1999;37:2754.
[30] Simha R, Wilson PS, Olabisi O. Kolloid-Z Z Polym 1973;251:402.
[31] Bondi AA. Physical properties of molecular crystals, liquids and glasses. New York: Wiley; 1968. Chapter 14.
[32] Simha R, Wilson PS. Macromolecules 1973;6:908.
[33] Kluin JE, Yu Z, Vleeshouwers S, McGerwey JD, Jamieson AM, Simha R, Sommer K. Macromolecules 1996;26:1853.
[34] Jean YC, Sandreczki TC, Ames DP. J Polym Sci, Part B: Polym Phys 1986;24:1247.
[35] Venditti RA, Gillham JK, Jean YC, Lou Y. J Coat Tech 1995;67:47.